

**MINISTRY OF EDUCATION  
AND TRAINING**

**VIETNAM NATIONAL  
CHEMICAL GROUP**

**VIETNAM INSTITUTE OF INDUSTRIAL CHEMISTRY**

**TRAN QUANG THIEN**

**KINETIC STUDY OF DDT DECOMPOSITION PROCESS BY  
ELECTROCHEMICAL AND CHEMICAL METHODS**

**MAJOR: THEORETICAL AND PHYSICAL CHEMISTRY**

**CODE: 62.44.01.19**

**SUPERVISOR: Ass. Prof. LE XUAN QUE**

**ABSTRACT OF DISSERTATION**

**HA NOI - 2018**

Reviewer 1:  
Reviewer 2:  
Reviewer 3:

The Dissertation will be defended before the Assessment Board at the Vietnam Institute of Industrial Chemistry at:

...h..., date..... month.....year 2018

The Dissertation can be accessed at:

- The National Library of Vietnam.
- The Library of Vietnam Institute of Industrial Chemistry.

## INTRODUCTION

DDT is one of the persistent organic pollutants (POP), and is used as pesticides (BVTV). However, there remains a large residual amount of DDT in Vietnam and in some other countries that used DDT in agriculture and wars. This severely makes harmful effects to the ecological environment, agricultural products, and especially human's health.

There have been several studies on how to decompose DDT in the world, such as electrochemically decomposing DDT in CH<sub>3</sub>CN solvent, or TMABFE electrolyte; or decomposing DDT by nano iron powder; by applying biological methods or physical methods, etc. However, studies on the kinetics of DDT decomposition are quite few, particularly the electrochemical and chemical kinetics of the decomposition process. Therefore, I choose the topic of *“Kinetic study of DDT decomposition process by electrochemical and chemical methods”* for my PhD dissertation.

### 1. Objectives of the dissertation

Overall objective: Examine the kinetics of the DDT decomposition process by electrochemical and chemical methods. More specifically:

- Examine the decomposition process of DDT by Cyclic Voltammetry method (CV) in the ethanol-water solvent.
- Examine the decomposition process of DDT by Potentiostatic (PS) polarization.
- Examine the kinetics of DDT decomposition process using iron power.
- Apply findings of the study to decompose DDT extracted from DDT contaminated soil in Hon Tro area.

### 2. Contents of the dissertation

- Study the kinetics of DDT decomposition process by CV methods to identify the decomposition reactions of DDT derivatives and the appropriate static potentials.
- Study the kinetics of DDT electrochemical decomposition process by PS method.
- Study the kinetics of DDT decomposition process in a solvent using iron metal powder.
- Apply the research findings to decompose DDT extracted from DDT contaminated soil in Hon Tro area using iron metal powder.

### 3. Scientific and practical meanings of the research topic

- Decomposition of DDT using iron metal powder produced at the Institute of Tropical Technology and Vietnam Academy of Science and

Technology is being studied to apply in the treatment of DDT contaminated soils. DDT is one of the POP that have direct harmful effects to the human's health, the environment and organisms. Therefore, the study on decomposition of DDT is necessary and highly practical.

- Study of the electrochemical decomposition of DDT in ethanol solvent contributes to the application of modern techniques in environmental treatment, helping to control the products of the decomposition process, and the solvent used is highly friendly with the environment.

#### **4. Contributions of the dissertation**

- The author has examined the DDT decomposition process by CV electrochemical method in the a solvent consisting of ethanol and  $\text{CaCl}_2$  electrolyte. Using differential technique, the author identifies 3 electrochemical reactions of the DDT decomposition process, equivalent to the three potentials of -0.46 V (DDT decomposition), -1.32 V (DDD decomposition) and -1.58 V, the limited potential  $E_{\text{gh}}$  of each reaction is chosen as the static potential; and results of the CV measurement is considered as the scientific base to choose the polarized potential PS.

- The potentiostatic polarization method used to decompose DDT gives good results.

- The author has identified the kinetics of the DDT decomposition reaction using iron powder in the laboratory:  $\ln C_{\text{DDT}} = -0,456.t + 4,677$ . Then the author has applied this result to decompose DDT extracted from contaminated soil in Hon Tro, which proves to be highly effective, reducing more than 90% of DDT content in the extracted solution.

#### **5. Structure of the dissertation**

The thesis has 108 pages in length, with 18 tables and 73 figures. It is structured as followed: Introduction: *3 pages*, Chapter 1: Literature review: *28 pages*, Chapter 2: Research methods and experiments: *13 pages*; Chapter 3: Results and discussion: *50 pages*, Conclusion: *1 page*. List of journal and conference papers: *1 pages*, References: *12 pages*.

## **MAIN CONTENTS OF THE DISSERTATION**

### **CHAPTER 1. LITERATURE REVIEW**

This chapter reviews national and international literatures on topics relating to the dissertation:

- 1.1. Plant protection products DDT
- 1.2. Iron metal powder
- 1.3. Decomposing organic compounds by iron metal powder
- 1.4. Electrochemical process to decompose organic compounds
- 1.5. Decomposing DDT by chemical and electrochemical methods

### **CHAPTER 2. EXPERIMENTS**

This chapter describes the experimental process of the dissertation.

#### **2.1. Chemicals and equipment**

#### **2.2. Research methodologies**

##### **2.2.1. Electrochemical method**

- Applying Cyclic Voltammetry (CV) and Potentiostatic methods to electrochemically decompose DDT.

##### **2.2.2. POP analysis method**

- Analyzing the content of DDT components by GC/MS system.

##### **2.2.3. Data analysis method**

- Using linear regression method to analyze data on excel 2007 and origin 9.0 soft wares.

#### **2.3. Steps of the experiments**

##### **2.3.1. Preparing the necessary solutions**

##### **2.3.2. Studying the electrochemical decomposition process of DDT by CV method**

- Examining the DDT decomposition process by CV methods, using solvents including M00, M0-01, M0-03, M0-05, M1 within a range of potentials of  $-2.1 \div 0.0V$ , scanning rate of  $10mV/s$ , and a potential jump of  $0.001V$ . Examining the electrochemical decomposition process of DDT and effects of electrolyte and water to its CV spectrum.

- Correlation between kinetic current of DDT decomposition and scanning rate: scanning CV in 3 cycles on 10ml M5, within a range of potentials of  $-1.65 \div 0.0V$ , scanning rate  $5mV/s$ ,  $10mV/s$ ,  $15mV/s$ , and a potential step of  $0.001V$ .

- Correlation between kinetic current of DDT decomposition and concentration: scanning CV in 3 cycles on 10ml M1, M2, M3, M4, M5, within a range of potentials of  $1.65 \div 0.0V$ , scanning rate  $10mV/s$ , and a potential step of  $0.001V$ .

##### **2.3.3. Studying the DDT decomposition process by Potentiostatic method**

- Examining the effects of static potential on the electrolytic solvent: Applying the polarized potential of  $-0.85V$  to the studied electrode, then measuring the responsive current  $i-t$  over time of 10 ml M0 and M6. Time for electrolyzation are 90, 120 and 150 minutes.

- Examining the effects of static potentials of -0.85V, -1.55V, -2.0V to the DDT decomposition process in 150 minutes.

### 2.3.4. Study the kinetics of DDT decomposition by chemical method

The decomposition reactions happen in 5 reactors, each containing 20 ml solvents composed of oxygen-removed reactants. Reaction time in each reactor are 1, 2, 4, 6 and 8 hours, respectively. When the reactions stop, content of DDT components are analyzed by centrifugal filter. The following experiments are conducted:

- Effects of pH: Experimenting with pH=3, 4 and 5.
- Effects of the surface area of iron: Experimenting with the content of iron powder of 3.5g/L, 7g/L and 10.5g/L.
- Effects of the stirring rate: Conducting the similar experiments with stirring rate of 50, 100 and 150 round/minute, respectively.

### 2.3.5. Decomposing DDT extracted from contaminated soil by iron metal powder

➤ Conducting similar experiments as described in section 2.3.4 on the solution extracted from contaminated soil with the content of 401.8g/L.

## CHAPTER 3. RESULTS AND DISCUSSION

### 3.1. Electrochemical decomposition of DDT by CV method

#### 3.1.1. Determining DDT decomposing reaction

Results of conductivity measurement of the solution with different contents of  $\text{CaCl}_2$  are presented in Table 3.1; and dependency of the conductivity on the content of the electrolyte is illustrated in Figure 3.1. The higher the content of  $\text{CaCl}_2$ , the higher the conductivity of the solution.

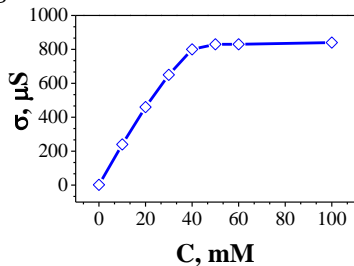
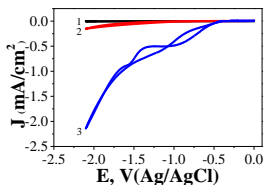


Figure 3.1. Dependency of the conductivity of the solvent on the content of  $\text{CaCl}_2$

Table 3.1. The conductivity of  $\text{CaCl}_2$  solution in  $\text{C}_2\text{H}_5\text{OH}$

Content of $\text{CaCl}_2$ (M)	0	0,01	0,02	0,03	0,04	0,05	0,06	0,1
Conductivity $\sigma$ ( $\mu\text{S}/\text{cm}$ )	1,5	240	460	650	800	830	835	840

The CV spectrum and cathode curves measured from sample M00, M0 and M1, first cycle, are illustrated in Figure 3.2 and 3.3.



**Figure 3.2.** The CV spectrum of solutions: 1 – M00, 2 – M0, 3 – M1.

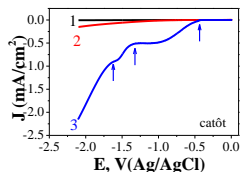


**Figure 3.3.** The Cathode curves and CV spectrum of solutions 1 – M00, 2 – M0, 3 – M1.

Evolution of the electrochemical processes with regard to the number of scanning cycles is illustrated in Figure 3.4. The evolution of cathode curve (Figure 3.5) and anode curve (Figure 3.6) with regard to scanning cycles show that, from cycle 1 to cycle 5, there all happen 3 electrochemical reactions.

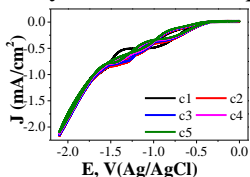


**Figure 3.4.** CV spectrum of cycle 1 to 5 of DDT.

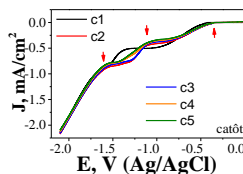


**Figure 3.5.** The cathode curve of cycle 1 to 5 of the CV spectrum of DDT.

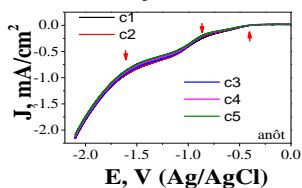


**Figure 3.6.** The anode curve of cycle 1 to 5 of CV spectrum of DDT.

However, at cycle 1, the evolution of the current and the reaction potential is different from those of the other cycles. Evidence is that only the cathode branch of cycle c1 has high decomposition current, while the subsequent cycles c2-c5 have high repetition levels (Figure 3.5 and 3.6).

### 3.1.2. The role of water to the ethanol solvent

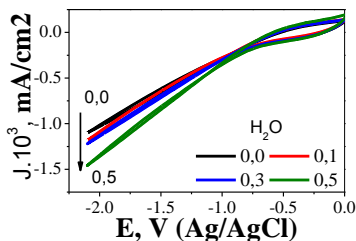


**Figure 3.7.** The CV spectrum measured in  $C_2H_5OH$  solution and  $C_2H_5OH+xH_2O$  at cycle 1. Scanning rate: 10mV/s, potential:  $-2.1 \div 0,0V$

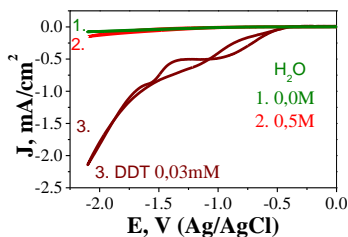


**Figure 3.8.** The CV spectrum measured in  $C_2H_5OH$  solution,  $C_2H_5OH+0.5M H_2O$  and DDT at cycle 1. Scanning rate: 10mV/s, potential:  $-2,1 \div 0,0V$ .

Intensity of the CV current of M00 with and without water are all as small as  $\mu\text{A}$  at the highest bias  $-2.1\text{V}$  and there appear no more cathode and anode pics when the content of water in the solution changes. This shows that water does not involve in the electrolytic process when scanning CV with ethanol solvent. With the sample M1, when the content of water increases to  $0.5\text{M}$ , it does not deform the CV curve (Figure 3.8).

### 3.1.3. Determining the potential and current of DDT decomposition reaction

#### 3.1.3.1. Identifying the DDT decomposition reaction

The bias spectrum of CV that examines the decomposing reaction of DDT derivatives, between sample that contains (M1) and not contain (M0) DDT has already been investigated in Figure 3.1. The measurement of CV spectrum of sample M1, cycle c1, is presented in Figure 3.9. However, the shape of the cathode curve in cycle c1 is different from those of the other 4 subsequent cycles (Figure 3.10).

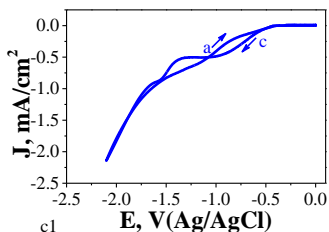


**Figure 3.9.** CV curve, cycle c1.

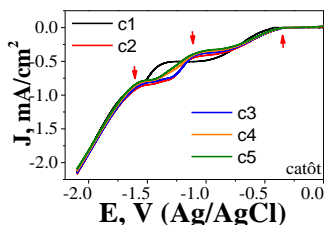


**Figure 3.10.** The cathode curves of CV spectrum from cycle c1 to c5, 4 curves from c2 to c5 have similar shapes.

Result of the differentiation of Cathode branch ( $dJ/dE$ ) is introduced in Figure 3.11. On the differential curve, it is easy to identify precisely three typical potentials for each reaction:  $E_{pu}$ , wave half potential  $E_{1/2}$  and limited potential  $E_{gh}$ . It is noted that  $E_{gh}$  of the previous reaction is the  $E_{pu}$  of the subsequent reaction:  $E_{gh}^1 = E_{pu}^2$ ;  $E_{gh}^2 = E_{pu}^3$

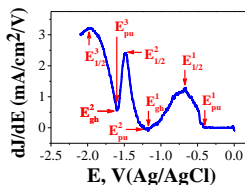


**Figure 3.11.** Derivative  $dJ/dE$  Cathode curve c1, 3, pic is the wave half  $E_{1/2}$  of 3 reactions 1-3.

#### 3.1.3.2. Xác định thế và dòng phản ứng 1

#### 3.1.3.2. Determining the potential and current of reaction 1

Results of the determination of reaction potential  $E_{pu}$ , limited potential  $E_{gh}$ , wave half potential  $E_{1/2}$  at different cycles of the reaction are presented in Figure 3.12 and Figure 3.13.

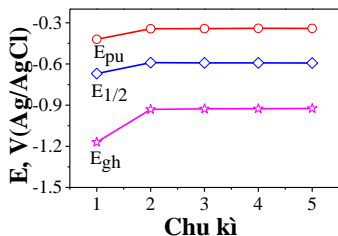


**Figure 3.12.** Changes in the typical potentials of reaction 1, cathode branch scanning at different cycles.

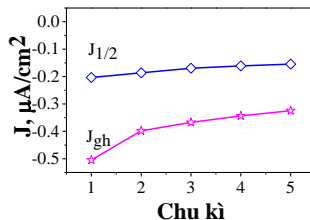


**Figure 3.13.** Changes in the values of typical current of reaction 1, cathode branch scanning at different cycles.

### 3.1.3.3. Determining the potential and current of reaction 2

Similar to reaction 1, results of the determination of the potential and kinetic current of reaction 2 are presented in Figure 3.14 and 3.15.

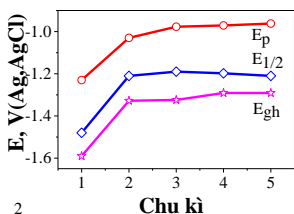


**Figure 3.14.** Changes in the typical potential of reaction 2, cathode branch scanning at different cycles.

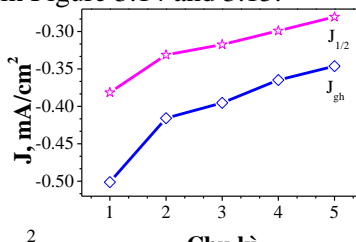


**Figure 3.15.** Changes in the values of typical current of reaction 2, cathode branch scanning at different cycles.

### 3.1.3.4. Determining the potential and current of reaction 3

Similar to reaction 1, results of the determination of the potential and kinetic current of reaction 3 are presented in Figure 3.16 and 3.17.

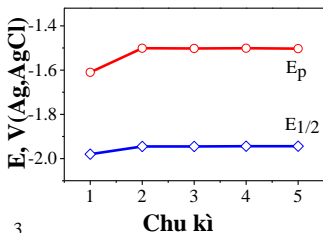


**Figure 3.16.** Changes in the typical potential of reaction 3, cathode branch scanning at different cycles.

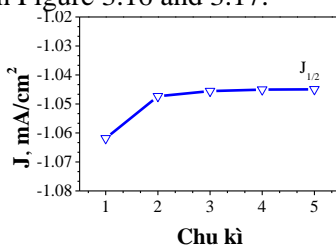


**Figure 3.17.** Changes in the typical current of reaction 3, cathode branch scanning at different cycles.

### 3.1.3.5. Comparing among decomposition reactions of DDT derivatives

From cycle c2, on the differential curve, 4 decomposing reactions can be recognized, which are characterized by 4 maximum  $dJ/dE$ . The new reactions are symbolized as 2', Figure 3.18. The appearance of reaction 2' on the  $dJ/dE$  E c2 shows that it might be a secondary reaction, products of the previous reaction, or even the reaction from cycle 1.

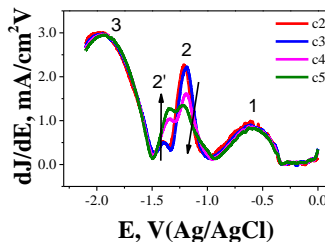


**Figure 3.18.** Differential  $dJ/dE$  cathode branch of CV spectrum, cycle c2 to c5.

### ❖ The typical current $J$ of each reaction

Changes in the kinetic current  $J$  of reaction from 1 to 3 with regard to the number of CV cycles are illustrated in Figure 3.19.

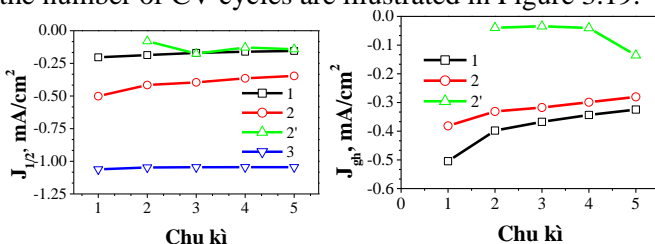


**Figure 3.19.** Changes in  $J_{1/2}$  and  $J_{gh}$  Cathode reaction with regard to the number of scanning cycle.

Similar to the reaction potential, cycle c1 has small kinetic current, after that it increases with the number of CV cycle, especially  $J_{gh}$ .

### 3.3.3.6. Discussion

There appear 4 electrochemical reactions in the decomposition process of DDT. It shows that the electrochemical decomposition process of DDT derivatives is a complex series of reactions. The decomposition process of DDT receives  $2e$  to become DDD, and this process is in line with reaction 1 determined on the bias curve CV. The second electrochemical process is identified as the decomposition process of DDD. Besides, reaction 2' might be the secondary reaction of the decomposition reactions of DDT and DDD.

### 3.1.4. Correlation between the decomposition current of DDT derivatives and the content and scanning rate

#### 3.1.4.1. Effects of the content of DDT

Results of the measurement of CV bias with different contents of DDT are presented in Figure 3.20. When the initial content of DDT increases, the intensity of cathode and anode currents all increase.

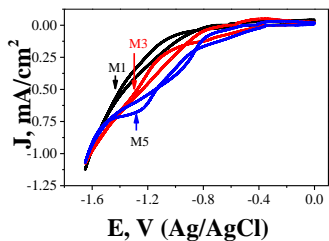


**Figure 3.20.** CV spectrum cycle 1, sample M1, M3, M5

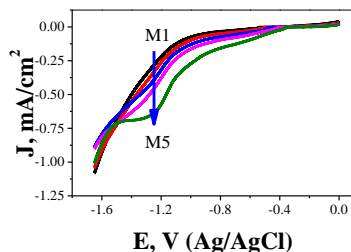


**Figure 3.21.** Cathode curve CV spectrum cycle 1, sample M1-M5

Dependency of the kinetic current of each reaction 1 and 2 on the content of DDT are illustrated in Figure 3.22.

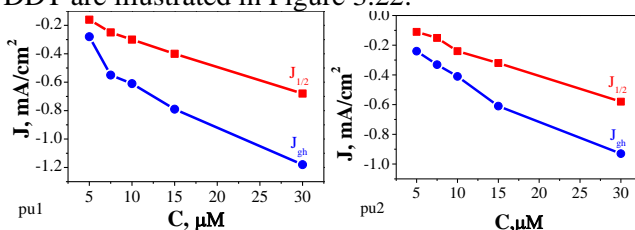


**Figure 3.22.** Dependency of the kinetic current on the content of DDT.

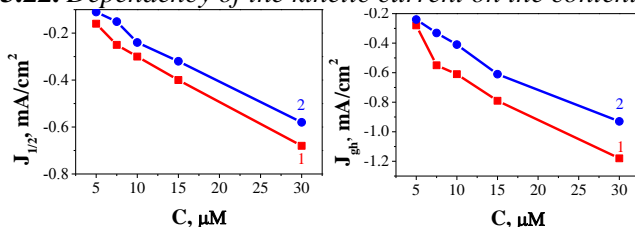


**Figure 3.23.** Comparing the kinetic currents of reaction 1 and 2, with different contents of DDT.

The content of DDT has large effect to the kinetic current, wave half current  $J_{1/2}$  and the limited current  $J_{gh}$ , which increase quickly when the content of DDT increases, Figure 3.23.

### 3.3.4.2. Impact of the scanning rate

The CV spectrum with different scanning rate are presented on Figure 3.24. With the scanning rate of 5mV/s, the intensity of the current is lowest. Kinetics currents of DDT decomposition reactions are determined on cathode branches. Figure 3.25 shows the cathode branch of cycle c1.

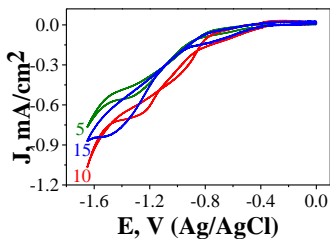


**Figure 3.24.** CV spectrum cycle 1 with different scanning rates.

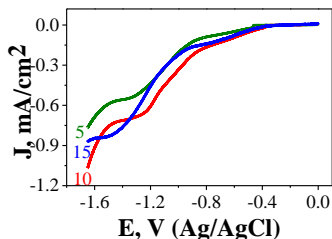


**Figure 3.25.** Cathode branch of CV spectrum, cycle c1, sample M5, different scanning rates.

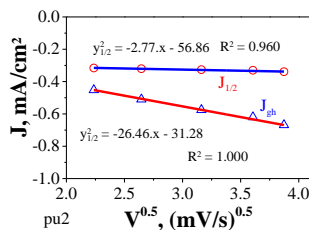
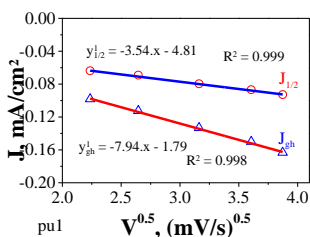


**Figure 3.26.** Dependency of the kinetic current  $J$  on  $v^{0.5}$ .

In reaction 1, wave half current follows function:  $y = -3,54.x - 4,81$ , correlation coefficient of  $R^2 = 0,999$ ; the limited current follows function:  $y = -7,94.x - 1,79$  and correlation coefficient of  $R^2 = 0,998$ . In reaction 2, wave half current follows function:  $y = -2,77.x - 56,86$ , correlation coefficient of  $R^2 = 0,960$ ; the limited current follows function:  $y = -26,46.x - 31,28$ , and correlation coefficient of  $R^2 = 1,000$ . (Figure 3.26).

### 3.2. Examining the decomposition process of DDT by potentiostatic method

#### 3.2.1. Electrochemical DDT reduction at static potential of -0.85V

At the static potential of -0.85V, and time for electrolyzation of 120 minutes, the responsive curves  $i-t$  when electrolyzing 10ml solvent M0 and 10ml solvent M6 are illustrated on Figure 3.27.

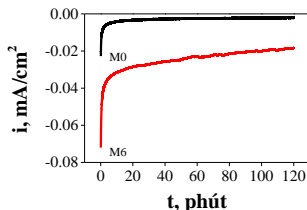


**Figure 3.27.** Responsive curves  $i-t$ , potential -0.85V, solvent M0, M6. 120 minute electrolyzation..

After sometime being electrolyzed (90, 120 and 150 mins) at a static potential of 0.85V, components of DDT (DDD, DDE, DDT) are analyzed on the solvent

sample. Results are presented in Table 3.2 and Figure 3.28. After increasing electrolyzation time, the content of DDT decreases while the contents of DDD and DDE increases. Changes in the content of DDE is very small compared to changes in DDT and DDD during the electrolyzation process. The results show that, at the potential of  $-0.85V$ , there happens an electrolyzation process of DDT. The decreases in the content of DDT, DDD and DDE after the 90, 120 and 150 minutes are presented in Figure 3.29.

Table 3.2. Contents of DDT components after electrolyzation, potential  $-0.85V$

Time (minutes)	Content (ppm)		
	DDT	DDD	DDE
0	176,10	15,71	4,38
90	159,28	31,11	4,62
120	157,18	32,78	4,92
150	153,14	36,81	5,12

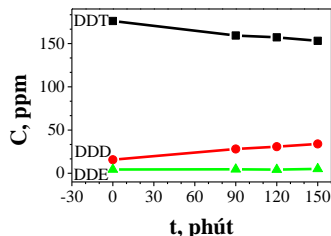


Figure 3.28. Contents of DDT, DDD, DDE after electrolyzation. Potential  $-0.85V$ .

Results show that, the larger the decrease in DDT content, the higher the increase in DDD content. The decline of DDE content increases by a very tiny scale, nearly equal to 0.

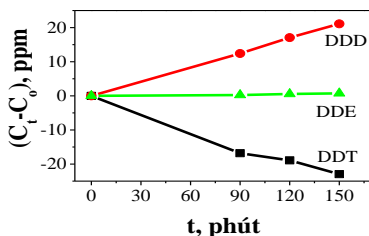


Figure 3.29. Decreases in the content of DDT components at different time of electrolyzation process. Static potential  $-0.85V$ .

These results show that, at the static potential of  $-0.85V$ , the formation and transformation of DDE through electrolyzation happens at a very small level. This is explained by Adi Setyo Purnomo *et al.* that during the decomposition process of DDT, DDD and DDE, there happens a mutual transformation according to the process illustrated in Figure 3.30. This means that, during the electrochemical decomposition process of DDT at the static potential of  $-0.85V$ , there happens a simultaneously process of chemical transformation in equilibrium on Figure 3.30.

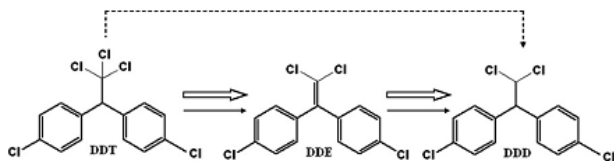


Figure 3.30. Transformation process of DDT, DDE and DDD [91].

### 3.2.2. Impacts of the electrochemical decomposition process to the ratios of the components of DDT

The percentage share of DDT components before and after electrolyzation are presented in Table 3.3. Dependency of the percentages of products on reaction time are illustrated on Figure 3.31.

Table 3.3. Percentage shares of DDT components over time

Time (min utes)	% content		
	DDT	DDD	DDE
0	89,76	8,01	2,23
90	81,68	15,95	2,37
120	80,65	16,82	3,4
150	78,51	18,87	2,62

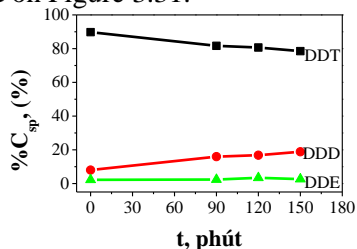


Figure 3. 31. Percentage shares of DDT, DDD and DDE after electrolyzation. Static potential  $-0,85V$ .

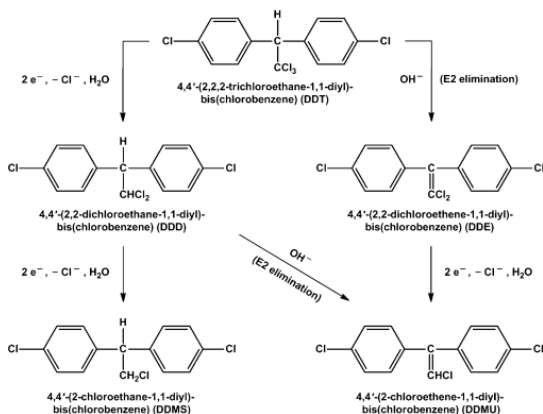


Figure 3.32. Transformation diagram of DDT [79].

### 3.2.4. Impacts of electrolysis potential to the shares of DDT components

Impact of the potential to the percentage shares of the products after 150 minutes electrolyzation are examined in a similar way as at the potential of  $-0.85V$ . The limited potentials ( $-0.85$ ;  $-1.55V$ ) of the reactions are determined in section 3.1 and the high potential is  $-2.0V$ . The contents of DDT, DDD and DDE at potential  $-1.55V$  and  $-2.0V$  are presented in Table 3.4. Changes in the content of DDT, DDD and DDE with regard to the electrolysis potentials are presented in Figure 3.34. Results show that, after 150 minutes electrolyzation, the content of DDT at different potentials are quite similar, and all smaller than the initial content of DDT. However, the contents of DDD and DDE at different potentials are not the same. Changes in the contents of DDT, DDD and DDE at different static potentials, and after 150 minutes electrolyzation are presented in Table 3.5. Changes in the

declines with regard to different potentials are presented in Figure 3.34.

*Table 3.4. Contents of DDT components at different potentials. Electrolyzation time is 150 minutes, initial content of DDT is 176.10; of DDD is 15.71, and of DDE is 4.38 ppm*

Potential (V)	Content (ppm)		
	DDT	DDD	DDE
-0,85	153,14	36,81	5,12
-1,55	152,91	13,66	30,38
-2,0	152,12	13,24	2,81

*Table 3.5. The decrease in the contents of DDT components at different potentials*

Potential (V)	$(C_t - C_0)$ (ppm)		
	DDT	DDD	DDE
-0,85	-22,96	21,1	0,74
-1,55	-23,19	-2,04	26,01
-2,0	-23,98	-2,47	-1,57

*Table 3.6. Percentage shares of DDT components at different potentials. Electrolyzation time is 150 minutes. The initial shares of the content of DDT, DDD and DDE are 89.76%, 8.01% and 2.23%, respectively*

Potential (V)	Percentage share (%)		
	DDT	DDD	DDE
-0.85	78.51	18.87	2.62
-1.55	77.63	6.94	15.43
-2.0	90.05	7.87	1.67

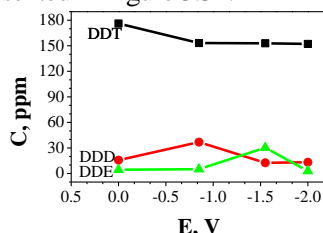


*Figure 3.33. Contents of DDT, DDD, DDE at different potentials. Electrolyzation time is 150 minutes.*

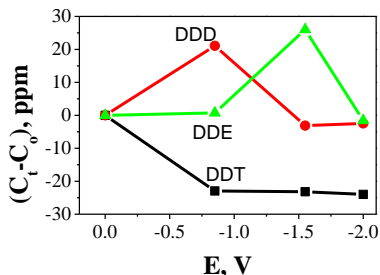


*Figure 3.34. The decrease in the contents of DDT components at different potentials. Electrolyzation time is 150 minutes.*

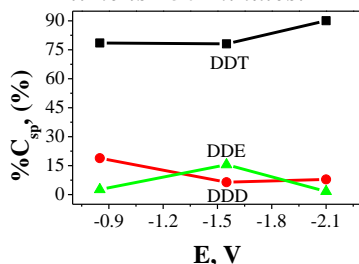


*Figure 3.35. Percentage shares of the contents of DDT, DDD and DDE at static potentials of -0.85V, -1.55V and -2.0V. Electrolyzation time is 150 minutes.*

The results show that, changes in the content of DDT, DDD and DDE at different potentials are different. The dependency of the percentage shares of DDT components on the static potential are presented in Figure 3.35. Efficiency of the decomposition process of DDT, DDD and DDE at different potentials, after 150 minutes electrolyzation are presented in Table 3.7. Figures reveal that, at the potential of -2.0V, the total efficiency of the decomposition of DDT reaches a peak of 65.23% because at this potential, there happens an electrolyzation process of DDT components, and the efficiency of the decomposition is highest. At the potential of -0.85V, the overall efficiency is lowest because there happens only the decomposition of DDT components in the solvent.

*Table 3.7. Efficiency of the electrolyzation process at different potentials, time length is 150 minutes. The initial content of DDT is 176.10; of DDD is 15.71 and of DDE is 4.38 ppm*

Potential (V)	Efficiency (%)		
	DDT	DDD	DDE
-0,85	13,04	-	-
-1,55	13,17	12,98	-
-2,0	13,67	15,72	35,84

### 3.3. KINETIC DECOMPOSITION OF DDT BY CHEMICAL METHOD

#### 3.3.1. Impacts of pH

##### 3.3.1.1. Examining the optimal pH condition

To find the optimal pH condition for the decomposition process of DDT by iron powder, we conduct experiments with different values of pH of 3, 4 and 5. Changes in the overall content of DDT when pH changes at different time points are presented in Table 3.8; and changes in the content of total DDT overtime are presented in Figure 3.36.

*Table 3.8. Changes in the content of total DDT when pH changes. Content of iron: 7g/L; stirring rate: 150 rpm*

pH value	Content of total DDT (mg/L)					
	0 hour	1 hour	2 hour	4 hour	6 hour	8 hour
3	100	73,44	55,82	30,93	13,95	6,74
4	100	86,35	68,70	42,94	25,09	18,04
5	100	93,33	77,57	51,88	33,97	25,94

Results show that, the content of total DDT decreases over time; but when pH increases, the content of total DDT after each time of reaction increases. At the same time of reaction, the content of total DDT changes

the most when pH increases from 3 to 4; and least when pH increases from 4 to 5.

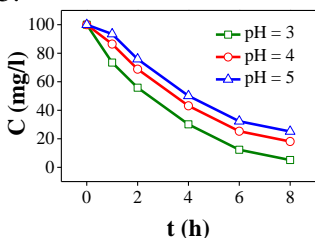


Figure 3.36. Content of DDT at different reaction time when pH changes.

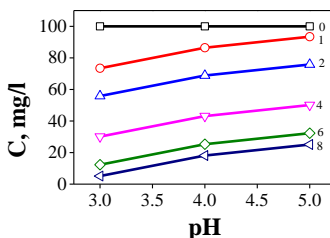


Figure 3.37. Changes in the content of total DDT with pH at different reaction time.

Results from Figure 3.36 show that, at each time of the reaction, the content of DDT changes differently. The rate of reaction is highest with pH=3, and lowest with pH=5.

When pH increases, the decomposition ability of iron power decreases. Efficiencies of the decomposition of total DDT over time with pH=3, 4, 5, respectively, are introduced in Figure 3.38.

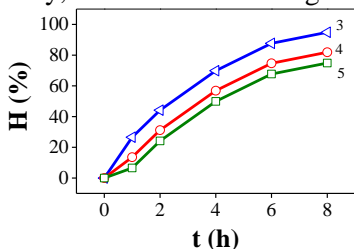


Figure 3.38. Efficiencies of DDT decomposition at time t, different pH values.

### 3.3.1.2. Impacts of pH on the kinetic reduction of DDT

❖ Kinetic function of the reaction

Dependency of  $\ln C_{DDT}$  on time t are presented in Figure 3.40.

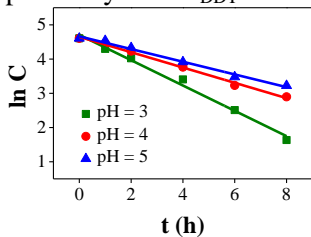


Figure 3.39. Dependency of  $\ln C_{DDT, pH}$  on t when pH changes.

At different time points, efficiencies of the reduction process of DDT when pH changes are different. The efficiency is highest within the first four hours, and in the next 4 hours, it falls sharply then becomes steady.

The equations expressing relationship between  $\ln C_{DDT, pH}$  and time t:

$$\ln C_{DDT, pH = 3} = -0,370.t + 4,706$$

$$R^2 = 0,989$$

$$\ln C_{DDT, pH = 4} = -0,224.t + 4,647$$

$$R^2 = 0,994$$

$$\ln C_{DDT, pH = 5} = -0,185.t + 4,663$$

$$R^2 = 0,988$$

❖ Average rate of total DDT decomposition

The average rates of the decomposition reaction are presented in Table 3.9 and the dependency of the average rate on time  $t$  is illustrated in Figure 3.40. Dependency of the average rate of DDT decomposition reaction with regard to different values of pH on the content of DDT at time  $t$  is presented in Figure 3.41.

Table 3.9. Average rate of DDT decomposition reaction over time. Content of iron powder: 7g/L, stirring rate: 150 rpm

pH value	Average rate (mg/Lh)					
	0 hour	1 hour	2 hours	4 hours	6 hours	8 hours
3	0	26,56	22,09	17,27	14,34	11,66
4	0	13,66	17,15	14,27	12,48	10,25
5	0	6,67	11,22	12,03	11,01	9,28

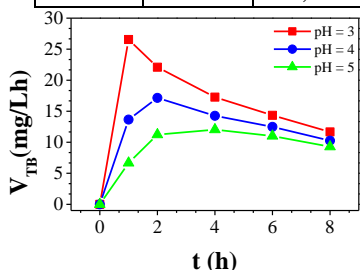


Figure 3.40. Dependency of the average rate of reaction on time  $t$ . Content of iron powder: 7g/L, stirring rate: 150 rpm.

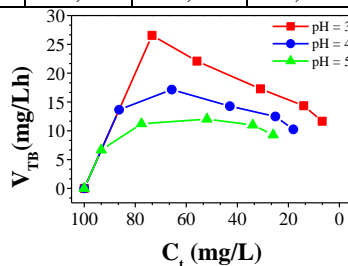


Figure 3.41. Dependency of the average rate of reaction on the content of DDT at time  $t$ . Content of iron: 7g/L; stirring rate: 150 rpm.

### 3.3.2. Impacts of the content of iron powder

#### 3.3.2.1. Examining the optimal condition

To determine the optimal content of iron powder and to evaluate the impacts of iron powder on the efficiency and the decomposition rate of 100mg/L DDT, we conduct experiments with the contents of iron powder of 3.5g/L, 7.0 g/L and 10.5g/L (equivalent to the area of contact with iron powder of 0.532; 1.064; 1.586  $m^2/L$ , respectively) in the non-oxygen condition to examine the rate of DDT decomposition reaction, pH=3, stirring rate: 150 rpm.

Table 3.10. Contents of total DDT when the content of iron powder in the solvent changes. Stirring rate: 150 rpm, pH=3

Content of iron powder (g/L)	Content of total DDT (mg/L)					
	0 hour	1 hour	2 hours	4 hours	6 hours	8 hours
3,5	100	85,24	70,82	45,12	27,38	20,21
7,0	100	73,44	55,82	30,25	12,29	5,12
10,5	100	65,34	43,82	18,14	8,23	2,96

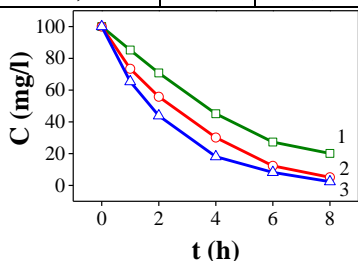


Figure 3.42. Content of DDT at different time of reaction; content of iron powder: 1 – 3,5g/L, 2 – 7g/L, 3 – 10,5g/L.

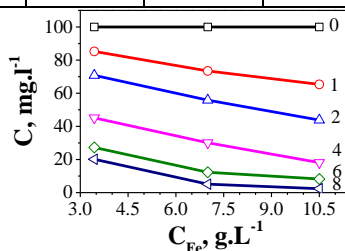


Figure 3.43. Changes in the content of total DDT responding to changes in the content of iron powder at different time of reaction.

Results show that, when the content of iron powder and reaction time increases, the content of total DDT decreases. At the same time of the reaction, when the content of iron powder increases, the content of total DDT decreases. At different time of the reaction, the decreases in the content of DDT are different.

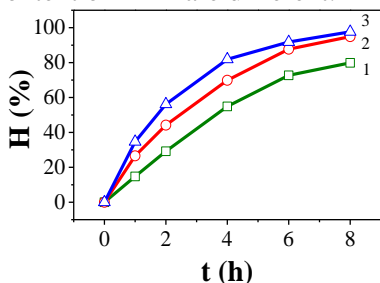


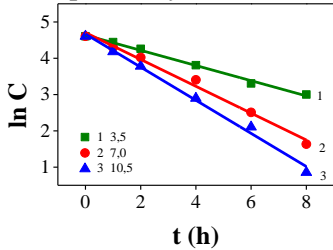
Figure 3.44. Decomposition efficiency of DDT at time t, with different contents of iron powder: 1 – 3,5; 2 – 7; 3 – 10,5g/L.

At different reaction time, efficiencies of the reduction process of DDT when the content of iron powder changes are different. The efficiency is highest within the first 4 hours. In the next 4 hours, it decreases then becomes steady. The efficiency is highest when the content of iron powder is 10.5g/L; and lowest when the content of iron powder is 3.5g/L.

### 3.3.2.2. Impacts of the content of iron powder on the kinetic decomposition of DDT

❖ Kinetic equation of the reaction

Dependency of  $\ln C$  on time  $t$  is presented in Figure 3.46.



The equations expressing the relationship between  $\ln C_{DDT, m}$  and time  $t$ :

$$\ln C_{DDT, 3,5} = -0,209.t + 4,637$$

$$R^2 = 0,994$$

$$\ln C_{DDT, 7,0} = -0,370.t + 4,706$$

$$R^2 = 0,989$$

$$\ln C_{DDT, 10,5} = -0,456.t + 4,668$$

$$R^2 = 0,992$$

Figure 3.45. Dependency of  $\ln C_{DDT, m}$  on time  $t$  when the content of iron powder changes.

Study on the dependency of the constant rate of reaction on the content of iron powder shows that, when the content of iron powder increases, the value of  $k'$  increases. Denoting  $S_{Fe}$  as the contact area of iron, the study shows that the constant  $k$  of the reaction is determined by this equation:  $k = k'/S_{Fe}$ . The values of  $k$  are presented in Table 3.11. The average rates of the DDT decomposition reaction with different contents of iron powder at different time  $t$  are presented in Table 3.12; and the dependency of the average rate of reaction are introduced in Figure 3.46. The dependency of the average rate of DDT reduction reaction with different contents of iron powder on the content of DDT at time  $t$  ( $C_i$ ) is presented in Figure 3.47.

Table 3.11. The constant rate of the transformation process of DDT with regard to the areas contacting with iron powder

Constant of the reaction	$S_{Fe}, m^2.L^{-1}$		
	0,532	1,064	1,596
$k'$	0,209	0,370	0,456
$k$	0,342		

❖ The average rate of total DDT decomposition over time

Table 3.12. Average rate of DDT decomposition reaction over time. Stirring rate: 150 rpm, pH=3

Content of iron powder (mg/L)	Average rate (mg/Lh)					
	0 hour	1 hour	2 hour s	4 hour s	6 hours	8 ho
3,5	0	14,76	14,59	13,72	12,10	9,97
7,0	0	26,56	22,09	17,27	14,34	11,66
10,5	0	34,66	28,09	20,47	15,29	12,13

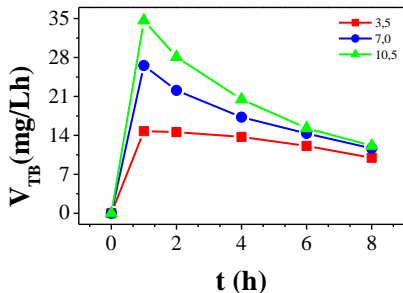


Figure 3.46. Dependency of the average rate of reaction on time  $t$ .  
Stirring rate: 150 rpm,  $pH=3$ .

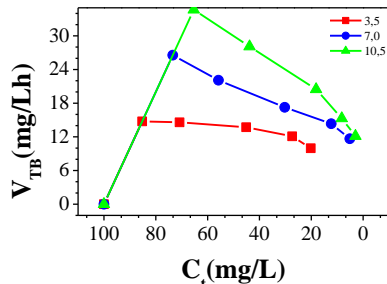


Figure 3.47. Dependency of the average rate of reaction on the content of DDT at time  $t$ . Stirring rate: 150 rpm,  $pH=3$ .

Figure 3.47 shows that, the average rate of DDT decomposition is lowest in all time with the content of iron powder of 3.5g/L; and is highest with the content of iron powder of 10.5g/L.

### 3.3.3. Impacts of stirring rate

#### 3.3.3.1. Examining the optimal condition

To examine the impacts of stirring rate to the kinetic decomposition of DDT, we conducts experiments with stirring rates of 50, 100 and 150 rpm, respectively. The contents of total DDT at different time points are presented in table 3.13 and the dependency of the content of DDT on time is illustrated in Figure 3.48. The contents of total DDT with different stirring rates and at different time points are presented in Figure 3.49.

Table 3. 13. Content of total DDT with different stirring rates. Content of iron powder: 10.5g/L;  $pH=3$

Stirring rate (round/minute)	Content of total DDT (mg/L)					
	0 hour	1 hour	2 hours	4 hours	6 hours	8 hours
50	100	86,44	68,82	43,12	29,29	19,12
100	100	83,35	61,80	35,03	17,20	11,02
150	100	65,77	44,35	18,06	7,95	2,96

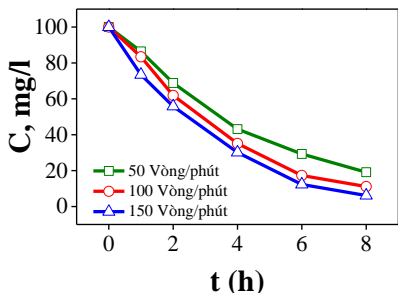


Figure 3.48. Content of DDT at different reaction time.

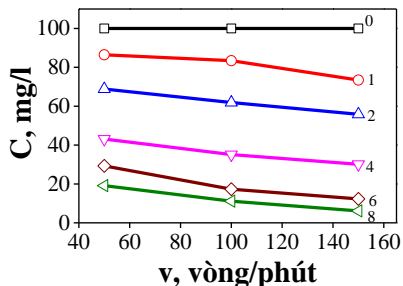


Figure 3.49. Changes in the content of total DDT following different stirring rates over time.

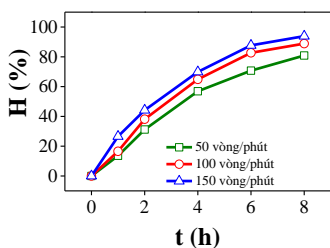


Figure 3.50. Efficiency of DDT reduction over time, different stirring rates.

At different time points, efficiency of the DDT reduction process changes when the content of iron powder changes. The efficiency reaches a peak within the first 4 hours of the reaction. In the next 4 hours, it decreases then become stable. With stirring rate of 150 rpm, the efficiency of the reaction is highest. And the efficiency is lowest with stirring rate of 50 rpm.

### 3.3.3.2. Impact of stirring rate on kinetic decomposition of DDT

#### ❖ Kinetic function of the reaction

Dependency of  $\ln C_{DDT}$  on time  $t$  is illustrated in Figure 3.52.

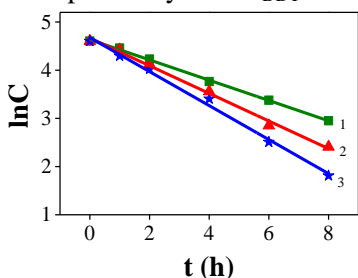


Figure 3.51. Dependency of  $\ln C_{DDT,v}$  on  $t$  when stirring rate changes..

Functions explaining the relationship between  $\ln C_{DDT, v}$  and time  $t$ :

$$\ln C_{DDT, 50} = -0,211.t + 4,636$$

$$R^2 = 0,998$$

$$\ln C_{DDT, 100} = -0,287.t + 4,666$$

$$R^2 = 0,994$$

$$\ln C_{DDT, 150} = -0,456.t + 4,668$$

$$R^2 = 0,992$$

#### ❖ Average rate of DDT decomposition

❖ The average rate of DDT decomposition changes when the stirring rate changes at each time of the reaction, which is presented in Table 3.14. Dependency of the average rate of reaction on time  $t$  is

illustrated in Figure 3.52. Dependency of the average rate of DDT reaction, with different stirring rate, on the content of DDT at time  $t$  is demonstrated in Figure 3.53.

❖ *Table 3.14. Average rate of DDT reduction over time. Iron powder: 10.5 g/L, pH = 3*

Stirring rate (round/minutes)	Average rate (mg/Lh)					
	0 hour	1 hour	2 hours	4 hours	6 hours	8 hours
50	0	13,56	15,59	14,22	11,79	10,11
100	0	16,65	19,10	16,24	13,80	11,12
150	0	34,66	28,09	20,47	15,29	12,13

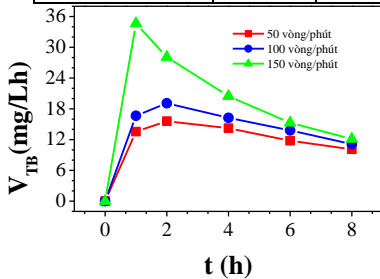


Figure 3.52. Dependency of average rate of reaction on time  $t$ . Iron powder: 10.5g/L, pH = 3.

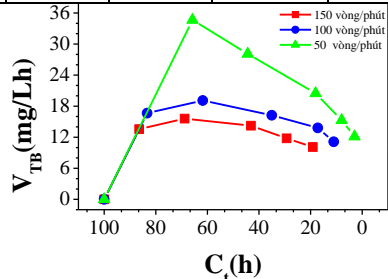


Figure 3.53. Dependency of average rate of reaction on the content of DDT at time  $t$ . Iron powder: 10.5g/L, pH = 3.

Kinetic functions of the DDT decomposition reactions in different conditions are introduced in Table 3.15.

*Table 3.15. Kinetic functions of DDT decomposition reaction*

Impact factors		Kinetic function	Slope
pH (iron powder: 7.0g/L, stirring rate 150 round/minutes)	3	$\ln C_{\text{DDT}, \text{pH}=3} = -0,370.t + 4,706$	-0,370
	4	$\ln C_{\text{DDT}, \text{pH}=4} = -0,224.t + 4,647$	-0,224
	5	$\ln C_{\text{DDT}, \text{pH}=5} = -0,185.t + 4,663$	-0,185
Content of iron powder (pH = 3, stirring rate 150 rpm)	3,5	$\ln C_{\text{DDT}, 3,5} = -0,209.t + 4,637$	-0,209
	7,0	$\ln C_{\text{DDT}, 7,0} = -0,370.t + 4,706$	-0,370
	10,5	$\ln C_{\text{DDT}, 10,5} = -0,456.t + 4,668$	-0,456
Stirring rate	50	$\ln C_{\text{DDT}, 50} = -0,211.t + 4,636$	-0,211

(pH = 3, iron powder 10.5 g/L)	100	$\ln C_{\text{DDT}, 100} = -0,287.t + 4,666$	-0,287
	150	$\ln C_{\text{DDT}, 150} = -0,456.t + 4,677$	-0,456

### 3.4. REDUCING DDT EXTRACTED FROM CONTAMINATED SOIL

Results of the experiments in section 3.3 are applied to decompose DDT extracted from contaminated soil in Hon Tro (Dien Chau, Nghe An) using iron powder. Changes in the content of DDT over time are introduced in Figure 3.54. Results show that, the contents of DDT, DDD and DDE are decreasing over time and get the highest falling rate within the first four hours, and the efficiency of decomposition reaches 69.85% (Figure 3.55).

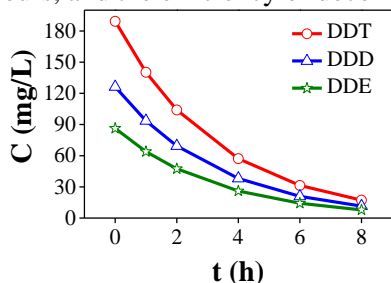


Figure 3.54. Content of DDT at different reaction time.

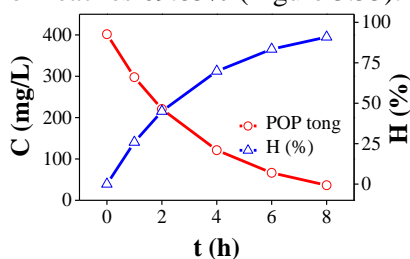


Figure 3.55. The content of total DDT and efficiency of the reaction at different time.

### CONCLUSION

This dissertation studies the kinetic decomposition of DDT using electrochemical methods (CV and potentiostatic methods) in ethanol solvent with electrolyte  $\text{CaCl}_2$ . It also examines the kinetic decomposition of DDT by chemical method using ironic metal powder. Main findings of this dissertation are listed below.

- Decomposing DDT by CV methods shows that, the solvent ethanol and  $\text{CaCl}_2$  is suitable for the electrochemical decomposition of DDT with the appearance of 3 electrochemical reactions on the bias curve CV at three potentials:  $-0.46\text{V}$  (reducing DDT),  $-1.32\text{V}$  (reducing DDD) and  $-1.58\text{V}$ . The limited kinetic current and limited potential of these reactions are identified as:
  - Decomposition reaction of DDT has  $J_{\text{gh}} = -0.505\text{mA/cm}^2$ ,  $E_{\text{gh}} = -0.85\text{V}$ .
  - Decomposition reaction of DDD has  $J_{\text{gh}} = -0.331\text{mA/cm}^2$ ,  $E_{\text{gh}} = -1.55\text{V}$ .
- Decomposing DDT by polarizing in 150 minutes at static potential  $E_{\text{PS}}$ , in which  $E_{\text{PS}} = E_{\text{gh}}$ , gives high electrolysis efficiency. At  $E_{\text{PS}} = -2.0\text{V}$ ,  $H = 65.23\%$ . At  $E_{\text{PS}} = -0.85\text{V}$ .

3. Decomposing DDT sample in the laboratory using iron powder at pH=3, stirring rate of 150 rpm in 8 hours, the decomposition efficiency reaches 97.04%, and the apparent kinetic of the reaction is order 1.
4. Applying research results to reduce DDT extracted from contaminated soil in Hon Tro using iron powder (which is produced at Institute of Tropical Technology) gets high efficiency rate, reaching 90.91%, meeting the current requirements on treatment of contaminated soil.
5. Results of the static potential polarization allow the application of electrochemical method at high bias potential, from -2.0V, to decompose DDT and its derivatives in DDT contaminated solvent.
6. Results from the study of decomposing DDT by electrochemical and chemical methods (using iron powder) prove that Vietnam can conduct DDT decomposition to revert contaminated soil using domestic technologies.

## LIST OF JOURNAL ARTICLES RELATING TO THIS DISSERTATION

1. **Trần Quang Thiện**, Nguyễn Quang Hợp, Lê Xuân Quế (2016), “Determining the potential and current of DDT decomposition reaction on the bias curve CV”, *Journal of Analytical Sciences*, vol. 3, pp. 85-92, 2016.
2. **Trần Quang Thiện**, Lê Xuân Quế (2016), “Studying the relationship between the kinetic current of decomposition of DDT derivatives and the content of DDT and scanning rate in CV method”, *Journal of Analytical Sciences*, vol. 4, pp. 80-86, 2016.
3. **Trần Quang Thiện**, Trần Thị Huyền, Lê Xuân Quế (2016), “Decomposing pesticides containing DDT remaining in contaminated soil using nano iron powder”, *Journal of Chemistry and Applications*, vol. 1, pp. 29-32, 2016.
4. Nguyễn Quang Hợp, **Trần Quang Thiện**, Dương Quang Huân, Nguyễn Văn Bằng, Lê Xuân Quế (2015), “Study on separating persistent organic pollutants (POP) remaining in soil by extracting water with QH<sub>2</sub> additive”, *Journal of Chemistry*, T.53(4E1), Tr.1-4, 2015.
5. **Trần Quang Thiện**, Nguyễn Quang Hợp, Dương Quang Huân, Nguyễn Văn Bằng, Lê Xuân Quế (2015), “Decomposing plant protection products extracted from contaminated soil”, *Journal of Chemistry*, số T.53(5e3), Tr.99-102, 2015.
6. Nguyễn Quang Hợp, **Trần Quang Thiện**, Dương Quang Huân, Nguyễn Văn Bằng, Lê Xuân Quế (2015), “Study on the influence of additives to the extracting and cleaning of soil contaminated with persistent organic pollutants”, *Journal of Chemistry*, số T.53(5e3), Tr.103-106, 2015.
7. **Trần Quang Thiện**, Lê Xuân Quế, “Study on the decomposition of DDT by potentiostatic method”, *Journal of Chemistry* (forthcoming).



